



## Wear Behavior of Al-Al<sub>3</sub>V and Al-(Al<sub>3</sub>V-Al<sub>2</sub>O<sub>3</sub>) Nanostructured Composites Fabricated by Mechanical Alloying and Hot Extrusion

Seyede Zahra Anvari<sup>\*1,2</sup>, Mohammad Hosein Enayati<sup>2</sup>, Fathallah Karimzadeh<sup>2</sup>

<sup>1</sup>Department of Mechanical Engineering, Payame Noor University (PNU), Tehran, Iran.

<sup>2</sup>Department of Materials Engineering, Isfahan University of Technology, Isfahan, Iran.

Received: 8 August 2020; Accepted: 8 October 2020

\* Corresponding author email: [szanvari@pnu.ac.ir](mailto:szanvari@pnu.ac.ir)

### ABSTRACT

The present work was undertaken to characterize the wear behavior of nanostructured Al-Al<sub>3</sub>V and Al-(Al<sub>3</sub>V-Al<sub>2</sub>O<sub>3</sub>) composites produced by milling and hot extrusion. The samples were characterized by pin-on-disk wear test, X-ray diffraction (XRD), and scanning electron microscopy (SEM). Results of wear test showed the nanostructured composites, as compared with the base metal, exhibited higher wear resistance. Dominate wear mechanism of the composites was recognized to be formation of mechanically mixed layer (MML) on the worn surfaces. Comparison of wear behavior of the Al-10 wt. %Al<sub>3</sub>V and Al-10 wt. %(Al<sub>3</sub>V-Al<sub>2</sub>O<sub>3</sub>) composites showed that Al-10 wt. %Al<sub>3</sub>V composite at different temperatures and for different loads has less wear rate than the Al-10 wt. %(Al<sub>3</sub>V-Al<sub>2</sub>O<sub>3</sub>) composite due to the weaker bond strength between Al<sub>2</sub>O<sub>3</sub> particles and Aluminum matrix.

**Key words:** *Wear, Aluminum, Metal matrix composite, Nanostructured materials, Mechanical alloying, Hot extrusion.*

### 1. Introduction

Aluminum alloys show attractive properties, such as low weight, relatively high specific strength, high corrosion resistance, making them of interest for automotive and aerospace industry [1]. However, the tribological properties of Al are influenced by its low hardness and the ease of oxidation [2-4]. In the past decades, incorporation of intermetallic and ceramic particles has been found to improve the wear resistance of Aluminum to a great extent. Aluminum metal matrix composites reinforced by hard particles have a high potential for automobile, aircraft and other applications components due to the excellent properties, such as specific strength, specific stiffness, and elastic module [5]. The wear resistance of the composites is mainly affected by the type, size, shape of the reinforcements and the

interfacial bonding strength with the matrix [6].

There are many routes, which are capable of fabricating Aluminum metal matrix composites. These methods can be considered as liquid-phase methods [7-9] and solid-state methods [10,11]. Among these methods powder metallurgy technique has found wide acceptance due to the attractive properties. This method results in a uniform distribution of the reinforcement particles without the segregation commonly found in cast composites [12]. In the past two decades, the wear resistance of aluminum alloys reinforced with SiC and Al<sub>2</sub>O<sub>3</sub> in many forms (particles, whiskers and fibers) and sizes has been described by a huge body of publications [13]. A good amount of work has been done on wear behavior of Aluminum composites reinforced with hard particles such

as  $\text{Al}_2\text{O}_3$  [14-16, 17], SiC [9, 18, 19],  $\text{TiB}_2$  [20],  $\text{B}_4\text{C}$  [7,8, 21],  $\text{ZrO}_2$  [22- 24],  $\text{SiC-TiO}_2$  [25]. But There are a few studies in literature which have reported the wear behavior of Al-based composites reinforced with  $\text{Al}_3\text{V}$ .

In previous study [26], Aluminum based nanostructured composites containing  $\text{Al}_3\text{V}$  and  $\text{Al}_3\text{V-Al}_2\text{O}_3$  reinforcement particles were produced through mechanical alloying and hot extrusion, and their mechanical properties were analyzed. In present study, the effect of reinforcement particles on wear behavior of the Aluminum based composites at ambient and high temperatures was explored.

**2. Materials and methods**

The raw materials used in this research were Aluminum powder (with a purity of 99.7% and a particle size smaller than 100  $\mu\text{m}$ ), vanadium powder (with a purity of 99.99% and a particle size smaller than 100  $\mu\text{m}$ ), and  $\text{V}_2\text{O}_5$  powder (with a purity of 99.99% and a particle size smaller than 5  $\mu\text{m}$ ). To produce the nanostructured Al-10 wt. %  $\text{Al}_3\text{V}$ , Al-10 wt. % ( $\text{Al}_3\text{V-Al}_2\text{O}_3$ ) composites and Al, mechanical alloying and hot extrusion were carried out. Flowchart of composite fabrication process is shown in Fig. 1. Ref. [26] presents details of the process and specifications of equipment. Dry sliding wear tests were carried out under ambient temperature using pin on disk wear testing machine. As prior to testing, the samples were firstly ground against number 1200 SiC grit papers, washed thoroughly with ethanol, dried, and then weighed using electric balance. The wear tests were performed under the loads of 25, 35, and 45 N. The total sliding distance was determined in 1000 m at a sliding speed of 0.12 m/s. The pin for this study was selected from samples produced in accordance with ASTM G99-04. The counter face disk was made from AISI 52100 steel with the hardness of 800 HV. High-temperature wear test was carried out at 200 and 400°C using a pin on disc wear testing device. The device was equipped with a furnace placed around the pin and disc for the wear test. Since the load-bearing test was not feasible at high temperature due to the microstructural changes resulted from the repeated increase and decrease in temperature, the wear test was conducted using the optimum wear load information at the ambient temperature (25 N). Linear velocity of hot wear was 0.1 m/min and the disc was an AISI 52100 steel disc with a

hardness of 800 HV.

X-ray diffractometry was used to evaluate the structural changes of samples. A Philips diffractometer (40 kV) with  $\text{Cu K}_\alpha$  radiation ( $\lambda=0.15406 \text{ nm}$ ) was used for XRD measurements. Scanning Electron Microscope (SEM) (Seron) equipped with energy dispersive X-ray spectroscopy (EDS) was used to study and analyze the morphologies of worn surfaces and wear debris.

**3. Results and discussion**

**3.1. Room temperature wear**

Fig.2 shows variation of volume loss with sliding distance for the nanostructured Al- $\text{Al}_3\text{V}$  composite and the wear rates obtained under the 25, 35 and 45 N loads. The strain hardening of the Aluminum matrix induced the decrement of mass loss rate. So, in long distances the wear rate is approximately invariant, which reflects a uniform decrease in the mass of the worn surface [27, 28].

Fig. 3 shows the SEM micrograph of worn

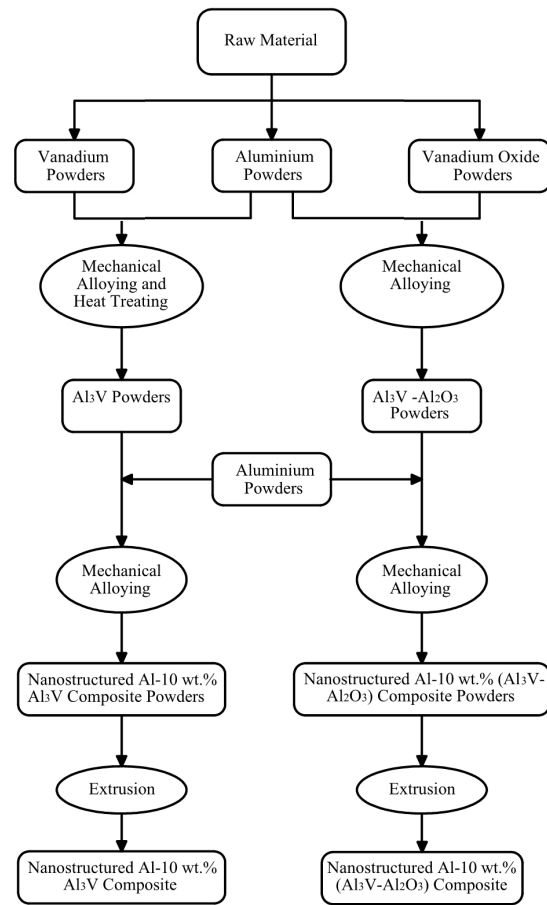


Fig. 1- Flowchart of composite fabrication process [26].

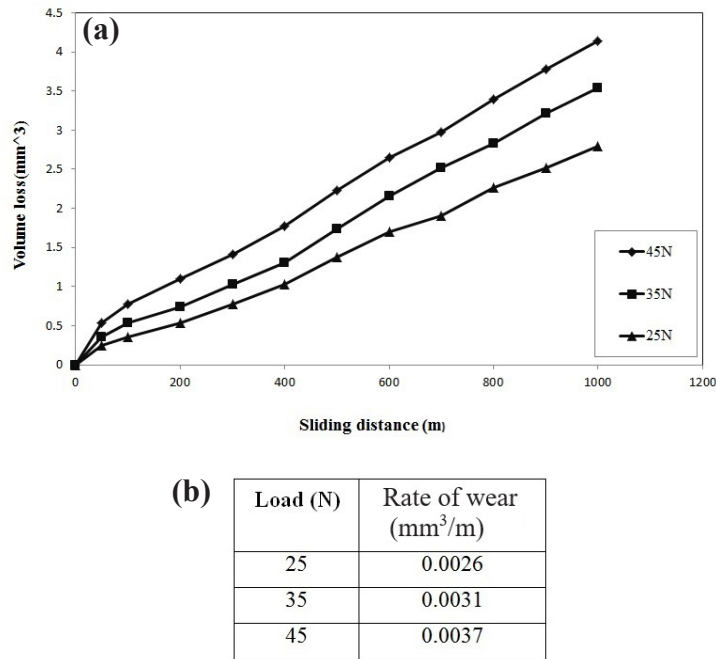


Fig. 2- (a) Wear volume loss data, and (b) rate of wear of the Al-Al<sub>3</sub>V composite.

surfaces of the Al-Al<sub>3</sub>V composite. As seen, uniaxial particles are present in the concavities. To further examine this sample, the EDS analysis was performed. Fig. 3 (b) shows the EDS analysis of the Al-Al<sub>3</sub>V composite worn surface. It seems that Fe is transferred from the steel disc to the worn surface. In addition, the presence of oxygen is due to oxidation of the surface during the wear process. Results of the EDS analysis are reflective of formation of a mechanically mixed layer (MML) between the composite surface and the steel disc during the wear process [12, 29]. This layer is Fe- and oxygen-rich, and formation of different oxidation phases in this layer results in a decrease of the wear rate [30]. Such results were obtained by other investigators previously [12, 20, 31-32]. Seemingly, the wear control mechanism in this composite is the formation of the mechanically mixed layer, delamination of this layer, and its reformation with continuation of the wear process.

Fig. 4 shows the SEM micrograph of the wear debris of the Al-Al<sub>3</sub>V composite in the beginning and end of wear process. As seen, the particles at the early stages of the wear process (Fig. 4 (a)) have a layered microstructure and metallic shine, which are indicative of delamination of wear debris [33]. As the wear process continues over a longer period of time, the particles deform into a combination of

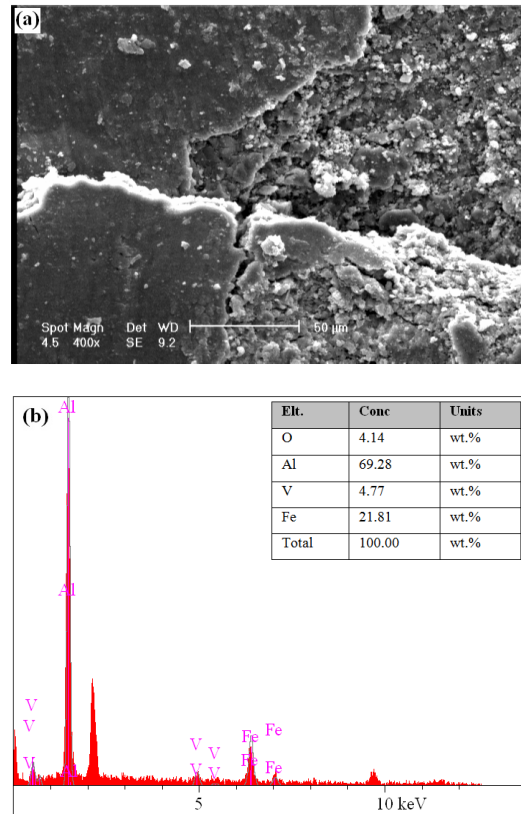


Fig. 3- (a) SEM micrograph of worn surface of the Al-Al<sub>3</sub>V composite, and (b) its corresponding EDS analysis.

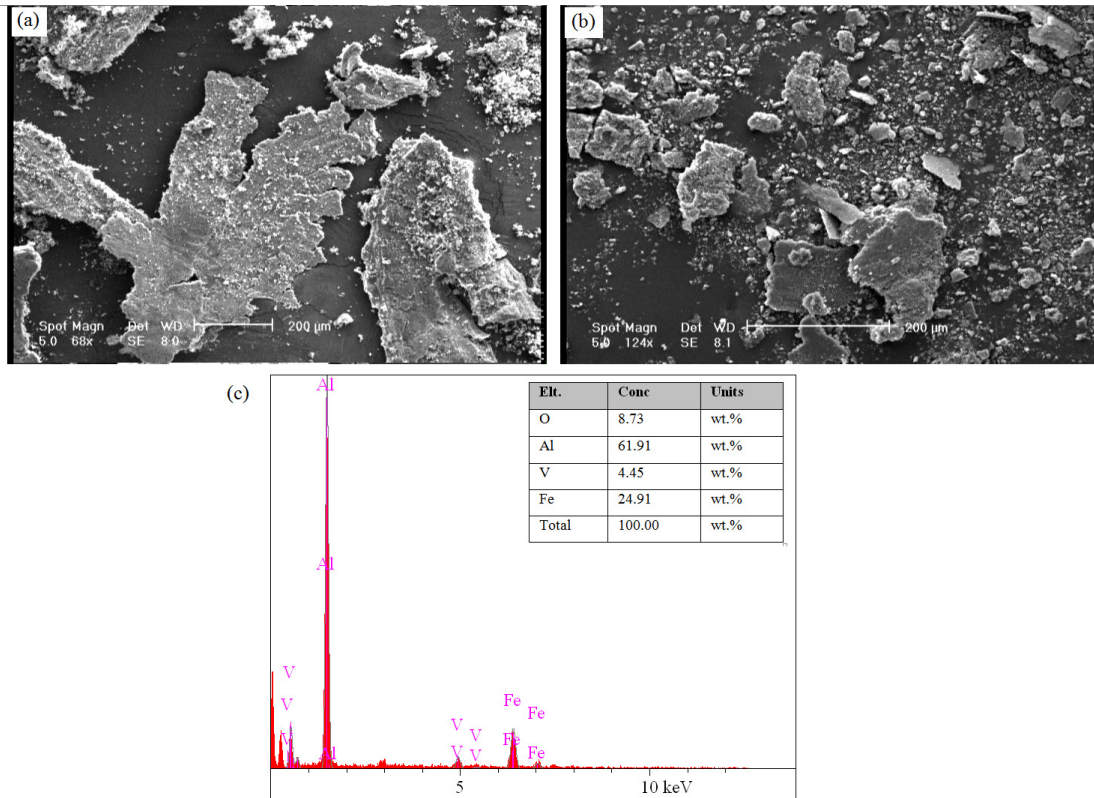


Fig. 4- SEM micrograph of wear debris of the Al-Al<sub>3</sub>V composite, (a) the early stages, (b) the end of process, and (c) EDS analysis of wear debris collected at the end of the process.

uniaxial fine particles and layered particles (Fig. 4 (b)). As mentioned, the mass loss rate was high in the beginning of the process, and the large size of wear debris and the absence of Fe and oxygen are reflective of this trend. As the process continues and the mechanically mixed layer forms, the high hardness of this layer results in a decrease in the wear rate and the particles resulting from the wear process display a small morphological form. Fig. 4(c) shows the results of the EDS analysis of wear debris collected at the end of the process. The chemical analysis of final wear debris and mechanically mixed layer are similar, therefore, it could be concluded that these particles were separated from this layer during the wear process.

The wear characteristic curves and mean wear rates of the nanostructured Al-(Al<sub>3</sub>V-Al<sub>2</sub>O<sub>3</sub>) composite are shown in Fig. 5 under the 25, 35 and 45N loads. The comparison between the wear rates of Al-(Al<sub>3</sub>V-Al<sub>2</sub>O<sub>3</sub>) composite (Fig. 5) and those of Al-Al<sub>3</sub>V composite (Fig. 2) under different loads reveals that the wear rate of the Al-(Al<sub>3</sub>V-Al<sub>2</sub>O<sub>3</sub>) composite is higher than the Al-Al<sub>3</sub>V

composite. Fig. 6 (a) shows the SEM micrograph of worn surface of Al-(Al<sub>3</sub>V-Al<sub>2</sub>O<sub>3</sub>) composite under the 35N load. Similar to Al-Al<sub>3</sub>V composite, the flat and concave regions are present on the worn surface of this sample. Fig. 6 (b) presents results of the EDS analysis of Al-(Al<sub>3</sub>V-Al<sub>2</sub>O<sub>3</sub>) composite under the 35 N load. These results are indicative of the presence of oxygen, Fe, and Al on the worn surfaces of this composite, which is a characteristic of the mechanically mixed layer.

SEM images of the worn surface of the nanostructured Aluminum under the 35 N load are shown in Fig. 7. The sample surface has displayed plastic deformation as a result of the wear process. In addition, the metal flow caused by the severe plastic deformation, which is a sign of the adhesive wear mechanism, is properly depicted. In addition, the parallel grooves on the worn surface indicate that the adhesive worn surface is accompanied by the abrasive wear mechanism. Fig. 8 depicts the wear debris of the nanostructured Aluminum. The wear debris also shows the flow and transfer of metal layers. Parallel abrasions are evident on the

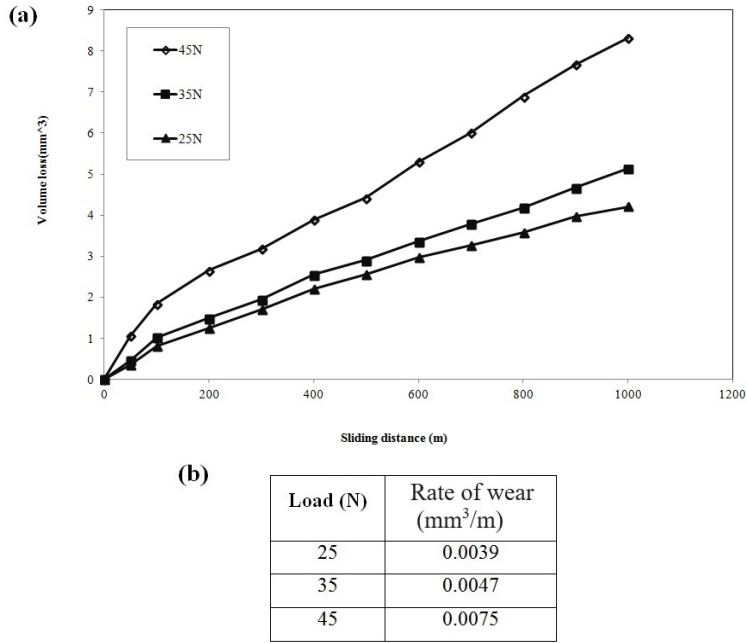


Fig. 5- (a) Wear volume loss data, and (b) rate of wear of the Al-(Al<sub>3</sub>V, Al<sub>2</sub>O<sub>3</sub>) composite.

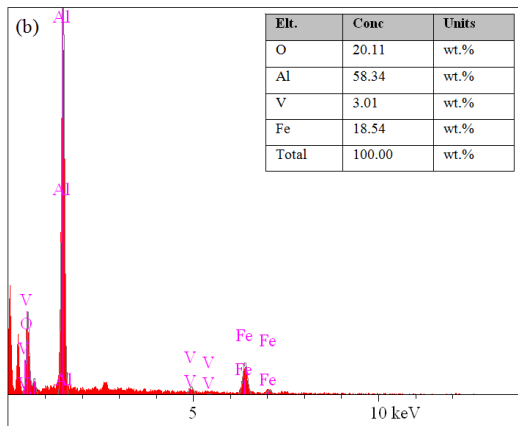
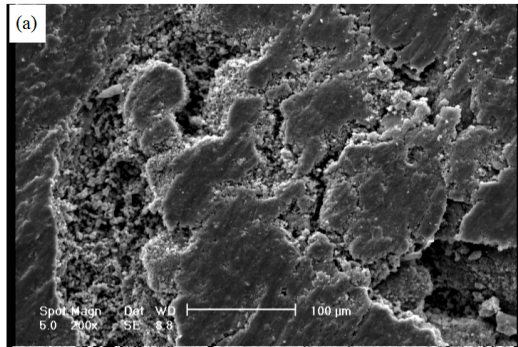


Fig. 6- (a) SEM micrograph of worn surface of the Al-(Al<sub>3</sub>V, Al<sub>2</sub>O<sub>3</sub>) composite, and (b) its corresponding EDS analysis.

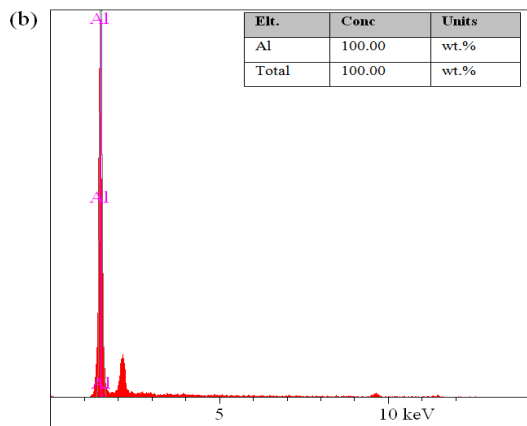
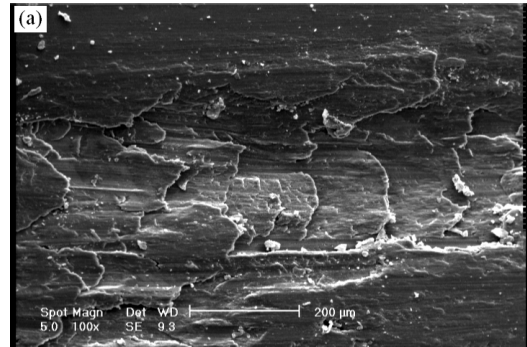


Fig. 7- (a) SEM micrographs of the worn surface of the nanostructured Aluminum, and (b) its corresponding EDS analysis.

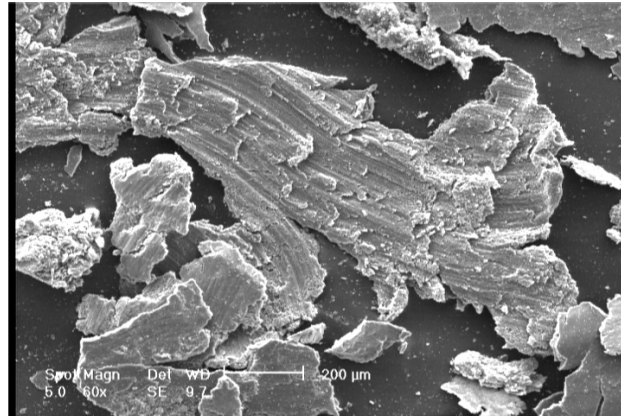


Fig. 8- SEM micrograph of wear debris of the nanostructured Aluminum.

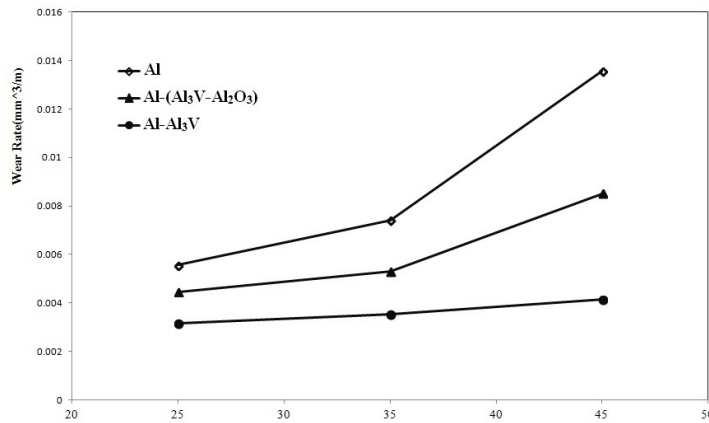


Fig. 9- Wear rate vs load of the composites and nanostructured Aluminum.

particles. The wear debris confirms the existence of the abrasive and adhesive mechanisms. The same adhesive wear mechanism in Aluminum based samples was reported by Kumar et al. [34] and by Alizadeh et al. [12].

Research results suggest that the presence of reinforcement particles plays a key role in formation of the mechanically mixed layer [16, 35]. Therefore, the worn surface of the nanostructured Aluminum was exposed to the EDS analysis. As seen in Fig.7 (b), only Aluminum is observed in the EDS analysis of this sample.

The wear rates of samples under different loads are shown in Fig. 9. As seen, as the applied load increases the wear rate of the composite samples escalates gradually, but the wear rate of the nanostructured Aluminum sample increases drastically. In addition, under all of the load conditions, the sample containing the Al<sub>3</sub>V reinforcement displays the highest wear resistance

and the nanostructured Aluminum shows the minimum wear resistance.

As mentioned, the wear mechanism of the composites under all loads was formation of an MML layer. A comparison between the wear rates of nanostructured Aluminum and the composites (Fig. 9) reveals that the wear rate in the nanostructured Aluminum is extremely higher than the composites. These results show the role of the MML layer in reducing the wear rate. MML layer acts as a protective layer due to its hardness (which is caused by the presence of Fe and Al oxides) and improves wear resistance of composites as compared to the nanostructured Al [20].

The comparison between the wear rates of the nanostructured Al-Al<sub>3</sub>V and Al-(Al<sub>3</sub>V-Al<sub>2</sub>O<sub>3</sub>) composites shows that under all of the applied loads the wear rate of the composite containing the dual reinforcement particles (Al<sub>3</sub>V and Al<sub>2</sub>O<sub>3</sub>) is higher than that of the composite containing

Table 1- Room temperature mechanical properties and densities of samples [26]

Sample	Grain size of Al matrix (nm)	Relative Density (%)	Hardness (MPa)	Yield strength (MPa)	Ultimate strength (MPa)	Fracture strain (%)
Al	71	97	519	80	180	25
Al- Al <sub>3</sub> V	58	96.9	725	118	209	14
Al- (Al <sub>3</sub> V-Al <sub>2</sub> O <sub>3</sub> )	62	96.5	843	123	226	11

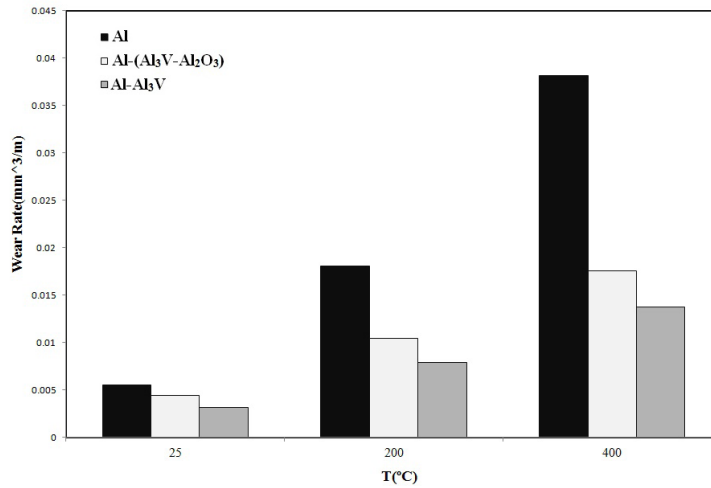


Fig. 10- Wear volume loss vs temperatures of the samples.

a single reinforcement (Al<sub>3</sub>V). According to the Archard equation, the dry sliding wear resistance of materials is proportional to their hardness [18]. While the hardness of Al-(Al<sub>3</sub>V-Al<sub>2</sub>O<sub>3</sub>) composite is higher than Al-Al<sub>3</sub>V composite (Table 1). Actually, hardness is not the only factor determining the wear rate of the composites, because the interfacial bonding between the matrix and the reinforcement also influences the wear rate [36]. The wear resistance of the metal-based composites depends on the type and properties of reinforcement particles, and the size, shape, distribution, and the bond between the particles and the matrix [22]. Although hardness of reinforcement particles increases the wear resistance in the composite, the strength of the bond between these particles and the matrix is significantly important [22]. A strong bond between the reinforcement particles and the matrix reduces pull out of particles and decreases three-body wear during the wear process [37]. To assess strength of the bond between the reinforcement particles and the matrix in the composites, a parameter known as the work of adhesion ( $W_{ad}$ ) is defined as the reversible work required for separating the surface unit of the interface between two phases [38]. This parameter can be obtained through eq. (1) and empirical

experiments or through theoretical calculations:

$$W_{ad} = \sigma_m + \sigma_p - \gamma_i \quad (\text{eq. 1})$$

Where,  $\sigma_m$  is the surface energy of matrix,  $\sigma_p$  is the surface energy of reinforcement particle, and  $\gamma_i$  is the energy of the matrix-reinforcement interface [39]. References reported values of 1078 [39] and 233mJ/m<sup>2</sup> [40] for the interface between Al-Al<sub>2</sub>O<sub>3</sub> and Al-Al<sub>3</sub>V, respectively. Given the difference in the  $W_{ad}$  values of the interface between Al-Al<sub>2</sub>O<sub>3</sub> and Al-Al<sub>3</sub>V, It seems the Al<sub>2</sub>O<sub>3</sub> reinforcement particles show a weaker bond to the Aluminum matrix than the Al<sub>3</sub>V reinforcement particles. Therefore, during the wear process, the alumina reinforcement particles separated from the composite containing two types of reinforcements acts as abrasive particles due to their higher hardness as compared to the matrix and lead to abrasion of both surfaces. Reduction of wear resistance due to pull out in metal matrix composites [41] and Al base composites [27, 7] have been reported.

### 3.2. High temperature wear

Fig. 10 shows the mean wear rate curves of the samples at different temperatures. As seen, the wear rate of the composites at different temperatures is extremely less than nanostructured Aluminum.

This difference becomes significant at the 400 °C temperature. The Aluminum matrix becomes softer at high temperatures and the applied load is transferred to the reinforcement particles. Hence, the composite wear resistance is determined by the reinforcement particles resistance to wear [42].

The SEM image of the worn surface of the Al-Al<sub>3</sub>V composite at the 200 and 400 °C temperatures is illustrated in Fig. 11. As seen, in spite of the increase in temperature of worn surface in this sample, its surface shows flat and concave areas similar to the worn surface observed at the ambient temperature (Fig. 3). The EDS analysis of the Al-Al<sub>3</sub>V composite worn surface at the 400 °C temperature (Fig. 11 (e)) confirms the presence of Fe. Hence, the mechanism governing wearing of this sample at high temperatures is formation of the MML layer.

Fig. 12 shows the worn surface of the nanostructured Al at 400 °C. As seen, the sample surface displayed severe plastic deformation during the wear process. The plastic deformations were so severe at some regions, that the worn surface of the sample was similar to a fractured surface with dimple. The intense metal flow under plastic deformations is indicative of an adhesive wear mechanism. Fig. 13 also shows the surface of the steel disc for the wear of this sample. As seen, the presence of Aluminum is observed on the surface of the disc. Therefore, the dominant wear mechanisms of nanostructured Aluminum at high temperatures are adhesive wear and melting wear mechanisms.

Fig. 14 shows the normalized wear rate (the wear rate of composite vs. the matrix wear rate) of the Al-Al<sub>3</sub>V and Al-(Al<sub>3</sub>V-Al<sub>2</sub>O<sub>3</sub>) composites at different

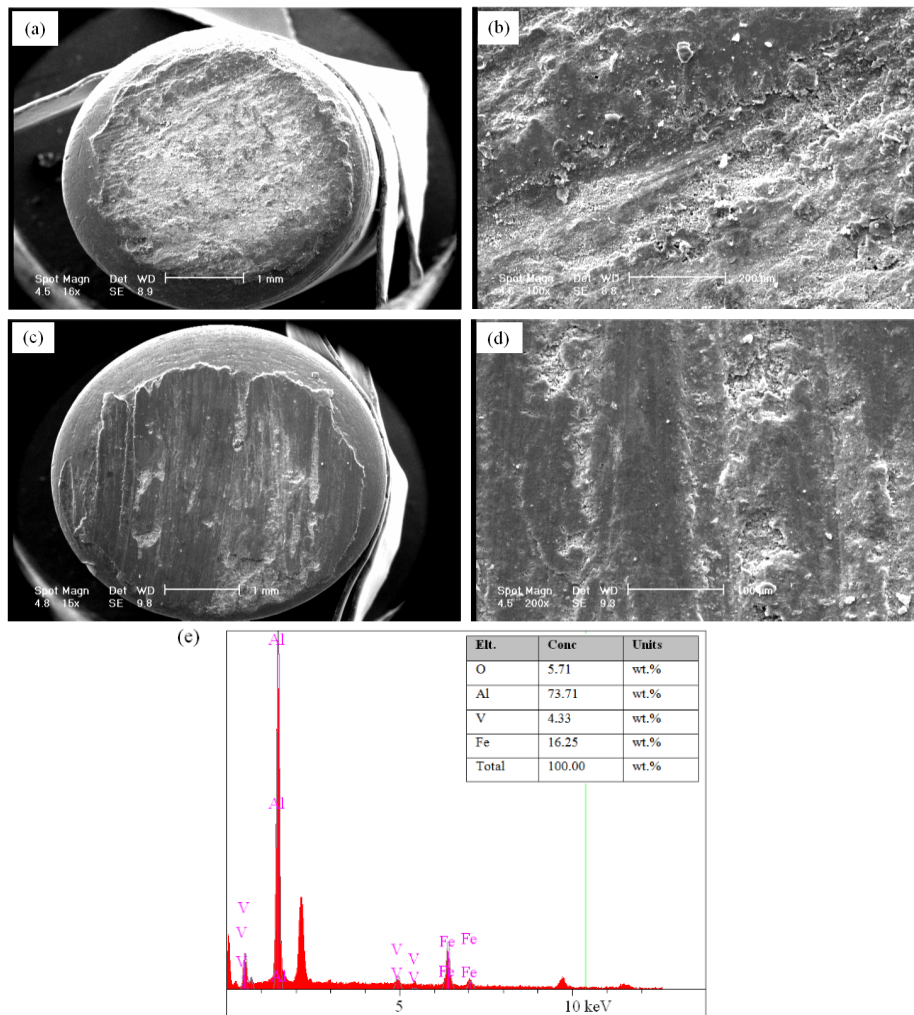


Fig. 11- The SEM image of the worn surface of the Al-Al<sub>3</sub>V composite at (a) and (b) 200 °C, (c) and (d) 400 °C and (e) EDS analysis of the worn surface at 400 °C.

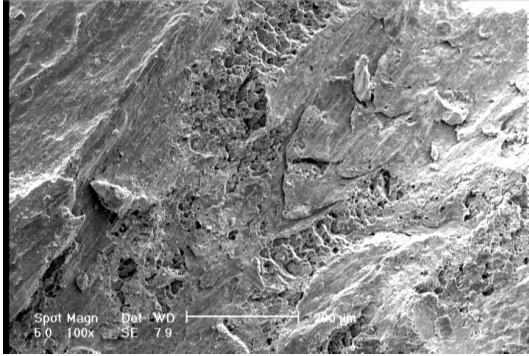


Fig. 12- The worn surface of the nanostructured Aluminum at 400 °C.



Fig. 13- The image of surface of the steel disc for nanostructured Aluminum at 200 °C.

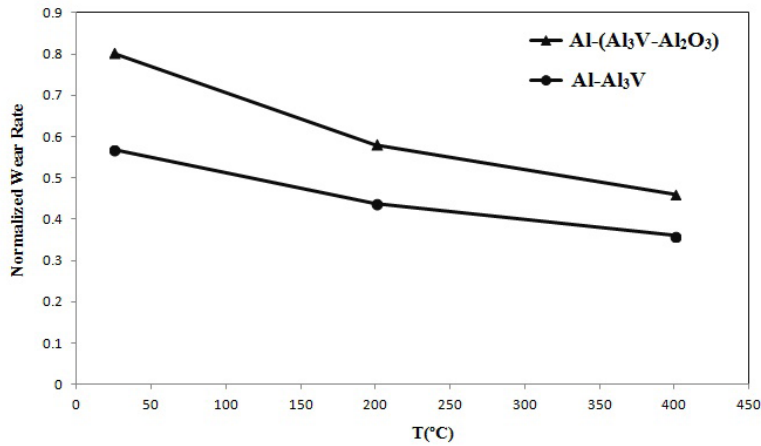


Fig. 14- The normalized wear rate of the Al-Al<sub>3</sub>V and Al-(Al<sub>3</sub>V-Al<sub>2</sub>O<sub>3</sub>) composites at different temperatures.

temperatures. As seen, in both composites the normalized wear rate decreases with an increase in temperature. This curve properly shows the greater effect of reinforcement particles on improvement of wear resistance at high temperatures. This effect can be attributed to the high thermal stability of reinforcement particles and the increase in thermal stability of composites. In the wear test, the Al matrix becomes softer with an increase in temperature and transfer of metal from the pin to the steel disc escalates (Fig. 13). However, presence of reinforcement particles in Aluminum matrix, reduces the tendency of matrix to soften. As a consequence, flow of metal from the sample surface subsides and wear resistance escalates as compared to the Aluminum matrix [31].

#### 4. Conclusions

The effect of reinforcement on the wear behavior of nanostructured Al-Al<sub>3</sub>V and Al-(Al<sub>3</sub>V-Al<sub>2</sub>O<sub>3</sub>) composites was studied. The following conclusions

were drawn:

- (1) The wear rate of nanostructured Al-Al<sub>3</sub>V and Al-(Al<sub>3</sub>V, Al<sub>2</sub>O<sub>3</sub>) composites decreased by 50 and 70%, respectively compared to the nanostructured Al.
- (2) A mechanically mixed layer containing a considerable amount of oxygen and Fe was formed on the worn surface of the composites. Formation of this layer seems to be a key factor in controlling the wear behavior of composites at high temperature.
- (3) The nanostructured Aluminum exhibited abrasive and adhesive wear at the ambient temperature and adhesive wear and melting wear at higher temperature.
- (4) Al-10 wt. % (Al<sub>3</sub>V-Al<sub>2</sub>O<sub>3</sub>) composite has a higher wear rate compared to Al-10 wt. % Al<sub>3</sub>V composite due to the weaker bond strength of Al<sub>2</sub>O<sub>3</sub> particles.
- (5) The presence of reinforcements further improves wear resistance of composites at high temperatures compared to ambient temperature.

## References

1. Choi S-H, Sung S-Y, Choi H-J, Sohn Y-H, Han B-S, Lee K-A. High Temperature Tensile Deformation Behavior of New Heat Resistant Aluminum Alloy. *Procedia Engineering*. 2011;10:159-64.
2. Le HR, Sutcliffe MPF, Wang PZ, Burstein GT. Surface oxide fracture in cold aluminium rolling. *Acta Materialia*. 2004;52(4):911-20.
3. Riahi AR, Alpas AT. The role of tribo-layers on the sliding wear behavior of graphitic aluminum matrix composites. *Wear*. 2001;251(1-12):1396-407.
4. Kim HJ, Emge A, Karthikeyan S, Rigney DA. Effects of tribooxidation on sliding behavior of aluminum. *Wear*. 2005;259(1-6):501-5.
5. Yu BC, Bae K-C, Jung JK, Kim Y-H, Park YH. Effect of Heat Treatment on the Microstructure and Wear Properties of Al-Zn-Mg-Cu/In-Situ Al-9Si-SiCp/Pure Al Composite by Powder Metallurgy. *Metals and Materials International*. 2018;24(3):576-85.
6. Zhu H, Min J, Li J, Chen J, Zhao J, Yao Y. Influence of B/ZrO2 molar ratios on the ambient temperature wear properties of composites made by an Al-ZrO2-B system. *Wear*. 2011;271(5-6):635-9.
7. Shorowordi KM, Haseeb ASMA, Celis JP. Tribo-surface characteristics of Al-B4C and Al-SiC composites worn under different contact pressures. *Wear*. 2006;261(5-6):634-41.
8. Lee KB, Sim HS, Kwon H, Kwon H, Cho SY. Tensile properties of 5052 Al Matrix composites reinforced with B4C particles. *Metallurgical and Materials Transactions A*. 2001;32(8):2142-7.
9. Lashgari HR, Zangeneh S, Shahmir H, Saghafi M, Emamy M. Heat treatment effect on the microstructure, tensile properties and dry sliding wear behavior of A356-10%B4C cast composites. *Materials & Design*. 2010;31(9):4414-22.
10. Mohanty RM, Balasubramanian K, Seshadri SK. Boron carbide-reinforced aluminium 1100 matrix composites: Fabrication and properties. *Materials Science and Engineering: A*. 2008;498(1-2):42-52.
11. Hajjhashemi M, Yazdian N, Karimzadeh F, Enayati MH. Physical, mechanical and dry sliding wear properties of hybrid and non-hybrid Al-V nanocomposites produced by powder metallurgy. *Powder Metallurgy*. 2017;60(4):309-20.
12. Alizadeh A, Taheri-Nassaj E. Mechanical properties and wear behavior of Al-2wt.% Cu alloy composites reinforced by B4C nanoparticles and fabricated by mechanical milling and hot extrusion. *Materials Characterization*. 2012;67:119-28.
13. Mahmoud ERI, Takahashi M, Shibayanagi T, Ikeuchi K. Wear characteristics of surface-hybrid-MMCs layer fabricated on aluminum plate by friction stir processing. *Wear*. 2010;268(9-10):1111-21.
14. Woo KD, Na HS, Kim SW, Sato T, Kamio A. Wear characteristics of Al-Si-Mg-(Cu)/Al2O3 composites fabricated by thermite reaction. *Metals and Materials International*. 2001;7(6):613-9.
15. Shehata F, Fathy A, Abdelhameed M, Moustafa SF. Preparation and properties of Al2O3 nanoparticle reinforced copper matrix composites by in situ processing. *Materials & Design*. 2009;30(7):2756-62.
16. Rosenberger MR, Forlerer E, Schvezov CE. Wear behavior of AA1060 reinforced with alumina under different loads. *Wear*. 2009;266(1-2):356-9.
17. Pournaderi S, Akhlaghi F. Wear behaviour of Al6061-Al 2 O 3 composites produced by in-situ powder metallurgy (IPM). *Powder Technology*. 2017;313:184-90.
18. Mosleh-Shirazi S, Akhlaghi F, Li D-y. Effect of SiC content on dry sliding wear, corrosion and corrosive wear of Al/SiC nanocomposites. *Transactions of Nonferrous Metals Society of China*. 2016;26(7):1801-8.
19. Prabhu Swamy NR, Ramesh CS, Chandrashekar T. Effect of heat treatment on strength and abrasive wear behaviour of Al6061-SiCp composites. *Bulletin of Materials Science*. 2010;33(1):49-54.
20. Mandal A, Murty BS, Chakraborty M. Wear behaviour of near eutectic Al-Si alloy reinforced with in-situ TiB2 particles. *Materials Science and Engineering: A*. 2009;506(1-2):27-33.
21. Abdollahi A. and Alizadeh A. A Tri-modal 2024 Al -B4C composites with super-high strength and ductility: Effect of coarse-grained aluminum fraction on mechanical behavior. *Journal of Ultrafine Grained and Nanostructured Materials*. 2014; 47-2:77-88.
22. Zhu HG, Ai YL, Min J, Wu Q, Wang HZ. Dry sliding wear behavior of Al-based composites fabricated by exothermic dispersion reaction in an Al-ZrO2-C system. *Wear*. 2010;268(11-12):1465-71.
23. Rostami RB, Tajally M. Effect of ZrO2 on microstructure and wear properties of Al2O3/Al-Si composites. *Emerging Materials Research*. 2017 Jan 23;6(1):160-7.
24. Ramachandra M, Abhishek A, Siddeshwar P, Bharathi V. Hardness and Wear Resistance of ZrO2 Nano Particle Reinforced Al Nanocomposites Produced by Powder Metallurgy. *Procedia Materials Science*. 2015;10:212-9.
25. Kumar CAV, Rajadurai JS. Influence of rutile (TiO2) content on wear and microhardness characteristics of aluminium-based hybrid composites synthesized by powder metallurgy. *Transactions of Nonferrous Metals Society of China*. 2016;26(1):63-73.
26. Anvari SZ, Karimzadeh F, Enayati MH. Synthesis and characterisation of nanostructured Al-Al3V and Al-(Al3V-Al2O3) composites by powder metallurgy. *Materials Science and Technology*. 2017;34(2):179-90.
27. Das S, Das S, Das K. RETRACTED: Abrasive wear of zircon sand and alumina reinforced Al-4.5 wt%Cu alloy matrix composites - A comparative study. *Composites Science and Technology*. 2007;67(3-4):746-51.
28. Hassan AM, Mayyas AT, Alrashdan A, Hayajneh MT. Wear behavior of Al-Cu and Al-Cu/SiC components produced by powder metallurgy. *Journal of Materials Science*. 2008;43(15):5368-75.
29. Li XY, Tandon KN. Microstructural characterization of mechanically mixed layer and wear debris in sliding wear of an Al alloy and an Al based composite. *Wear*. 2000;245(1-2):148-61.
30. Lu D; Gu M.; Shi Z. Materials transfer and formation of mechanically mixed layer in dry sliding wear of metal matrix composites against steel. *Tribology Lett*. 1999; 6:57-61.
31. Kumar S, Sarma VS, Murty BS. High temperature wear behavior of Al-4Cu-TiB2 in situ composites. *Wear*. 2010;268(11-12):1266-74.
32. Li XY, Tandon KN. Mechanical mixing induced by sliding wear of an Al-Si alloy against M2 steel. *Wear*. 1999;225-229:640-8.
33. Prasada Rao AK, Das K, Murty BS, Chakraborty M. Microstructure and the wear mechanism of grain-refined aluminum during dry sliding against steel disc. *Wear*. 2008;264(7-8):638-47.
34. Kumar S, Chakraborty M, Subramanya Sarma V, Murty BS. Tensile and wear behaviour of in situ Al-7Si/TiB2 particulate composites. *Wear*. 2008;265(1-2):134-42.
35. An J, Liu YB, Lu Y, Zhang QY, Dong C. Dry sliding wear behavior of hot extruded Al-Si-Pb alloys in the temperature range 25-200 °C. *Wear*. 2004;256(3-4):374-85.
36. Senthil Kumaran S.; Kumaresh Babu S.P.; Natarajan S.; Siva

- Prasad K. High Temperature Sliding Wear Behavior of Al 4032-ZrB<sub>2</sub> in situ Composite. *Int J Mat Sci*. 2009; 4:283–298.
- 37.Salvador MD, Amigó V, Martínez N, Busquets DJ. Microstructure and mechanical behaviour of Al–Si–Mg alloys reinforced with Ti–Al intermetallics. *Journal of Materials Processing Technology*. 2003;143-144:605-11.
- 38.Ibrahim IA, Mohamed FA, Lavernia EJ. Particulate reinforced metal matrix composites — a review. *Journal of Materials Science*. 1991;26(5):1137-56.
- 39.Smith JR, Zhang W. Stoichiometric interfaces of Al and Ag with Al<sub>2</sub>O<sub>3</sub>. *Acta Materialia*. 2000;48(18-19):4395-403.
- 40.Li J, Qi Y, Zhang M, Zhou Y, Li X. First-principle study of adhesion, wetting and bonding on Al/Al<sub>3</sub>V(001) interface. *Surface Science*. 2014;624:1-7.
- 41.Tjong SC, Wu SQ, Zhu HG. Wear behavior of in situ TiB<sub>2</sub>-Al<sub>2</sub>O<sub>3</sub>/Al and TiB<sub>2</sub>-Al<sub>2</sub>O<sub>3</sub>/Al–Cu composites. *Composites Science and Technology*. 1999;59(9):1341-7.
- 42.Fu H-H, Han K-S, Song J-I. Wear properties of Saffil/Al, Saffil/Al<sub>2</sub>O<sub>3</sub>/Al and Saffil/SiC/Al hybrid metal matrix composites. *Wear*. 2004;256(7-8):705-13.